



Quaternized chitosan (QCS)/poly (aspartic acid) nanoparticles as a protein drug-delivery system

Tie wei Wang^{a,b}, Qing Xu^a, Yan Wu^{a,*}, Ai jun Zeng^b, Mingjun Li^c, Hongxia Gao^c

^a National Center for Nanoscience and Technology, No. 11 Beiyitiao, Zhongguancun, Beijing 100190, China

^b China Agricultural University, Beijing 100083, China

^c The first affiliated Hospital of Jiamusi University, Jiamusi 154002, China

ARTICLE INFO

Article history:

Received 14 January 2009

Received in revised form 10 February 2009

Accepted 19 February 2009

Available online 25 February 2009

Keywords:

Quaternized chitosan

Poly (aspartic acid)

Nanoparticles

Protein

Delivery

ABSTRACT

The aim of this study was to generate a new type of nanoparticles made of quaternized chitosan (QCS) and poly (aspartic acid) and to evaluate their potential for the association and delivery of protein drugs. QCS and poly (aspartic acid) were processed to nanoparticles via the ionotropic gelation technique. The size, polydispersity, zeta potential, and morphology of the nanoparticles were characterized. Entrapment studies of the nanoparticles were conducted using bovine serum albumin (BSA) as a model protein. The effects of the pH value of nanoparticles with different QCS/poly (aspartic acid) ratios, QCS molecular weight (MW), poly (aspartic acid) concentration, and BSA concentration on the nanoparticle size, the nanoparticle yield, and BSA encapsulation were studied in detail. Suitably pH value of nanoparticles with different QCS/poly (aspartic acid) ratios, moderate QCS MW, optimal concentration ratio of poly (aspartic acid), and QCS favored more nanoparticles formed and higher BSA encapsulation efficiency. The release of BSA from nanoparticles was pH-dependent. Fast release occurred in 0.1 M phosphate buffer solution (PBS, pH 7.4), while the release was slow in 0.1 M HCl (pH 1.2). The results showed that the new QCS/poly (aspartic acid) nanoparticles have a promising potential in protein delivery system.

© 2009 Elsevier Ltd. All rights reserved.

1. Introduction

The physicochemical and biological properties of protein and peptide drugs (PPD) are different from those of conventional ones, such as molecular size, biological half-life, conformational stability, physico-chemical stability, solubility, oral bioavailability, dose requirement, and administration. Therefore, design and manufacturing of PPD delivery systems have been a challenging area of research. So far, some of conventional colloidal drug-delivery systems, such as liposomes and nanoparticles, have been developed and tested for PPD.^{1–3}

However, the bioavailability of peptide after oral administration is usually low due to instability and poor absorption of proteins in the gastrointestinal tract. One possible way to improve the gastrointestinal uptake of peptides is to encapsulate them in colloidal nanoparticles that can protect the peptide from being degraded in the gastrointestinal tract and facilitate their transportation into systemic circulation.^{4,5} It has been found that delivery systems with mean diameters in the range of hundreds of nanometers penetrated the epithelia more easily than the particles in the micrometer size range.^{6,7} Recently, the idea of using nanoparticles made from natural biodegradable polymers to de-

liver drugs has provoked great interest. Researchers found that synthetic biodegradable polymers, such as polyglycolic acid, polylactide, and their copolymers,^{8–10} were not ideal carriers for hydrophilic peptides and proteins, because of the strong hydrophobic property of those polymers. Moreover, the organic solvent used in the preparation procedure may reduce the biological activity of the protein.

Chitosan (CS) is the second most abundant polysaccharide in nature and a cationic polyelectrolyte present. CS has shown favorable biocompatibility characteristics as well as the ability to increase membrane permeability, both in vitro and in vivo, and be degraded by lysozyme in serum. CS has shown in different studies to prolong the residence time of drug-delivery systems at the site of drug absorption and is known to open transiently the tight junctions.^{11–18} But chitosan is only soluble in acid medium.¹⁹ In order to increase the stability of chitosan particles and avoid exposure to additional chemicals, the ionic gelation technique is useful. To overcome this demerit of chitosan, introducing quaternization on the chitosan backbone renders the polymer soluble over a wider pH range and confers controlled cationic property.²⁰ Quaternized chitosan, with improved solubility and enhanced positive charge intensity. It has been shown that quaternized chitosan (QCS) significantly enhanced the absorption across mucosal epithelia even in neutral environment.^{21,22} Owing to the good water solubility of QCS, it

* Corresponding author. Tel.: +86 10 82545614; fax: +86 10 62656765.

E-mail address: wuy@nanoctr.cn (Y. Wu).

is appealing to prepare peptide (protein) loaded with QCS-coated nanoparticles in neutral water phase.

Poly (aspartic acid) and its derivatives possess extensive applications in the field of biomedicine, due to their excellent biocompatibility and biodegradability, and have been reported to be mucoadhesive, biodegradable, and biocompatible and have potential for numerous pharmaceutical and biomedical applications such as drug-delivery systems and cell encapsulation.^{23–28} Recently the synthesis and application of polyaspartic acid has been studied in many companies. However, little work was focused on the complex of quaternized chitosan (QCS) and poly (aspartic acid).

Taking this information into account, the aim of this study was to combine the virtue of QCS and of poly (aspartic acid) in one drug-delivery system intended for the delivery of protein. We have developed nanoparticles made of CS and TPP and evaluated their ability to entrap hydrophilic drugs.²⁹ In this work, our idea was to obtain nanoparticles consisting of QCS and the anionic poly (aspartic acid) and to study the possibility to associate protein.

QCS/poly (aspartic acid) nanoparticles were prepared via the ionotropic gelation method. The resulting nanoparticles were characterized regarding their size, zeta potential, and shape. Nanoparticles were loaded with a protein model drug, BSA. Size, zeta potential, shape, stability, and drug release of resulting particles were determined *in vitro*.

The influence of the molecular factors of the cationic polymers on the formation and release of QCS/poly (aspartic acid) nanoparticles has been rarely investigated. In this study, we looked into the effects of pH value of nanoparticles with different QCS/poly (aspartic acid) ratios, QCS Mw, QCS concentration, poly (aspartic acid) concentration, and BSA concentration on the nanoparticle size, the nanoparticles yield and BSA encapsulation. The relationships among nanoparticle size, nanoparticles yield, and BSA encapsulation were to be studied. The release properties of BSA were also evaluated. Some experiments were done in order to optimize the encapsulation efficiency as a protein-delivery system and to modulate the release rate by adjusting the molecular and formation parameters.

2. Results and discussion

2.1. Preparation and characterization of QCS and QCS nanoparticles

The Scheme for the preparation of QCS/poly (aspartic acid) nanoparticles is shown in Figure 1.

Figure 2a and b shows the IR spectra of chitosan and quaternized chitosan (QCS) and identified the existence of quaternary amino groups on QCS chains. In the spectrum of QCS, the characteristic peak (1599 cm^{-1}) representing NH_2 deformation was weakened and a new peak positioned at 1483 cm^{-1} (belongs to the methyl groups in the ammonium) was made to appeared, which corresponded to an asymmetric angular bending of methyl groups of quaternary hydrogen. The characteristic peaks of primary alcohol and secondary alcohol between 1145 and 1081 cm^{-1} did not change in QCS comparing with chitosan that proved the introduction of quaternary amino groups at NH_2 sites on chitosan chains.

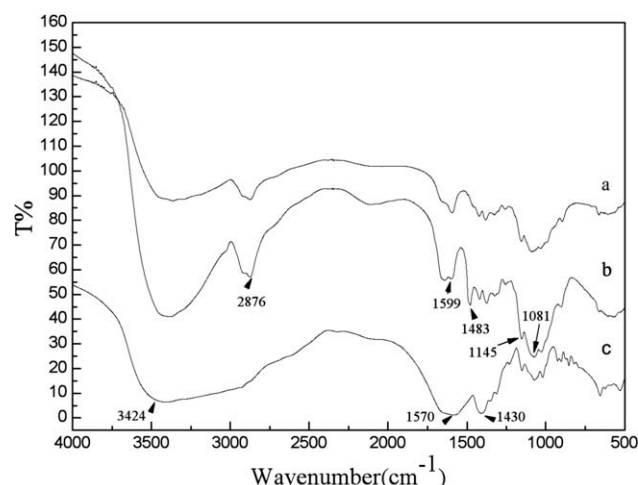


Figure 2. FT-IR spectra for (a) chitosan and (b) QCS and (c) QCS/ poly (aspartic acid) nanoparticles.

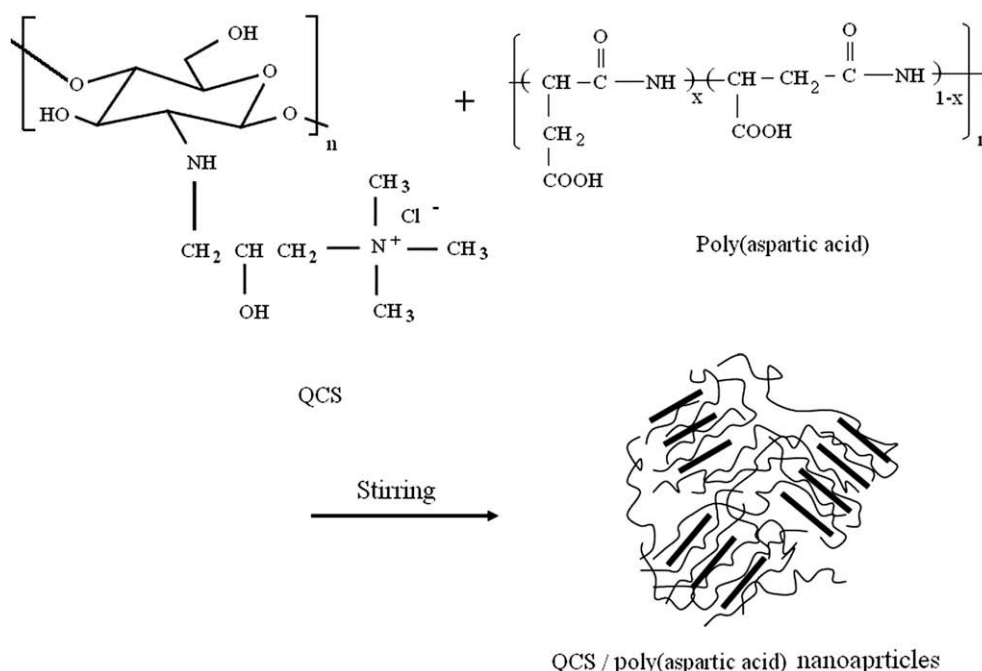


Figure 1. Scheme of the preparation of QCS/poly (aspartic acid) nanoparticles, (—) QCS, (—) poly (aspartic acid).

Nanoparticles of QCS/poly (aspartic acid) were prepared via the ionotropic gelation technique. This method utilizes the ionic interaction between the positively charged QCS and the negatively charged poly (aspartic acid), and the ability of QCS to form a gel after contact with polyanions by forming inter- and intramolecular linkages.

The spectrum of QCS/poly (aspartic acid) nanoparticles (Fig. 2c) is different from that of QCS matrix (Fig. 2b). In QCS/poly (aspartic acid) nanoparticles the peak of 3424 cm^{-1} ($\nu(\text{OH})$) became wider, indicating that hydrogen bonding is enhanced. In QCS/poly (aspartic acid) nanoparticles, the 1599 cm^{-1} peak of $-\text{NH}_2$ bending vibration shifts to 1570 cm^{-1} and the absorption peak of 2876 cm^{-1} disappeared. The new peak 1430 cm^{-1} (salt of carboxyl) appeared. The results indicated the presence of the electrostatic interactions between carboxyl groups of poly (aspartic acid) and $-\text{N}^+(\text{CH}_3)_3$ groups in QCS.

Figure 3A shows the morphological characteristics of nanoparticles. The nanoparticles were spherical in shape. Figure 3B shows the typical size distributions of QCS/poly (aspartic acid) nanoparticles. The size of these nanoparticles (determined by TEM) was smaller than that determined by DLS in water, presumably arising from the dry state of the TEM measurement. The zeta potential of nanoparticles was positively charged as measured, so we supposed that QCS surrounded the outer layer of the nanoparticles.

The ionic gelation process was extremely mild and involved the mixture of two aqueous phases at room temperature. The effects which included the pH value of nanoparticles with different QCS/poly (aspartic acid) ratios, QCS Mw, QCS concentration, poly (aspartic acid) concentration, and BSA concentration on the aver-

age particle size, polydispersity, zeta potential of the nanoparticles, nanoparticles yield, and BSA encapsulation efficiency were studied and the results are listed in Tables 1–5, respectively. The influences

Table 1

pH Value and zeta potential of nanoparticles with different QCS/poly (aspartic acid) ratios^a

QCS/poly (aspartic acid) ratios	pH Value	Zeta potential (mV)
1:1	6.02	49.18 ± 2.56
2:1	6.15	54.21 ± 2.89
4:1	6.31	60.21 ± 2.16
8:1	6.49	63.15 ± 2.89

^a The zeta potential of pure QCS was +65.9 mV, pH 6.58, QCS Mw = 65 kDa, $n = 3$.

Table 2

Effects of QCS M_w on the average particle sizes, polydispersity, and zeta potential values, and nanoparticle yield of QCS/poly (aspartic acid) nanoparticles^a

QCS M_w (kDa)	Average particle sizes (nm)	Polydispersity	Zeta potential values (mV)	Nanoparticle yield (mg)
65	205.8 ± 3.6	0.116 ± 0.07	54.21 ± 2.89	5.6 ± 0.01
80	224.6 ± 2.1	0.088 ± 0.07	55.2 ± 1.89	5.7 ± 0.02
110	247.8 ± 4.2	0.101 ± 0.07	56.4 ± 1.11	5.8 ± 0.01
142	261.9 ± 5.3	0.122 ± 0.07	57.2 ± 2.12	5.9 ± 0.02
230	310.1 ± 2.5	0.119 ± 0.07	58.1 ± 1.23	6.1 ± 0.01

^a QCS concentration = 2 mg/mL, poly (aspartic acid) concentration = 1 mg/mL, $n = 3$.

Table 3

Effects of QCS concentration on the average particle sizes, polydispersity, and zeta potential values and nanoparticle yield of QCS/poly (aspartic acid) nanoparticles^a

QCS concentration (mg/mL)	Average particle sizes	Polydispersity	Zeta potential values	Nanoparticle yield (mg)
1	188.1 ± 5.6	0.121 ± 0.01	48.21 ± 1.24	4.6 ± 0.01
2	205.8 ± 3.6	0.116 ± 0.02	54.21 ± 2.89	5.6 ± 0.01
3	337.4 ± 5.1	0.112 ± 0.01	61.4 ± 1.43	4.8 ± 0.01
4	385.9 ± 6.2	0.085 ± 0.02	60.2 ± 0.98	4.5 ± 0.02
5	433.6 ± 7.8	0.109 ± 0.03	56.7 ± 0.86	3.1 ± 0.02
8	462.3 ± 9.1	0.196 ± 0.03	57.5 ± 1.11	2.6 ± 0.01

^a Poly (aspartic acid) concentration = 1 mg/mL, QCS Mw = 65 kDa, $n = 3$.

Table 4

Effects of poly (aspartic acid) concentration on the average particle sizes, polydispersity and nanoparticle yield of QCS/poly (aspartic acid) nanoparticles^a

Polyaspartic acid concentration (mg/mL)	QCS concentration (mg/mL)	Average particle sizes	Polydispersity	Nanoparticle yield (mg)
0.5	2	138.1 ± 3.4	0.113 ± 0.01	2.8 ± 0.02
1	2	205.8 ± 3.6	0.116 ± 0.02	5.6 ± 0.01
1.5	2	347.5 ± 3.6	0.095 ± 0.02	8.8 ± 0.02
2	2	412.9 ± 2.4	0.129 ± 0.01	11.5 ± 0.01

^a QCS Mw = 65 kDa, $n = 3$.

Table 5

Effects of BSA concentration on the average particle sizes, polydispersity, and zeta potential values of QCS/poly (aspartic acid) nanoparticles^a

BSA concentration (mg/mL)	Average particle sizes (nm)	Polydispersity	Zeta potential values (mV)
0	205.8 ± 3.6	0.116 ± 0.02	54.21 ± 2.89
0.2	203.2 ± 2.1	0.177 ± 0.02	53.89 ± 1.66
0.5	187.6 ± 1.9	0.182 ± 0.02	53.96 ± 1.45
1.0	182.8 ± 3.2	0.185 ± 0.01	52.27 ± 1.72
1.5	165.9 ± 2.5	0.175 ± 0.01	51.33 ± 1.33
2.0	168.4 ± 3.3	0.211 ± 0.01	51.08 ± 1.11

^a QCS concentration = 2 mg/mL, poly (aspartic acid) concentration = 1 mg/mL, QCS Mw = 65 kDa, $n = 3$.

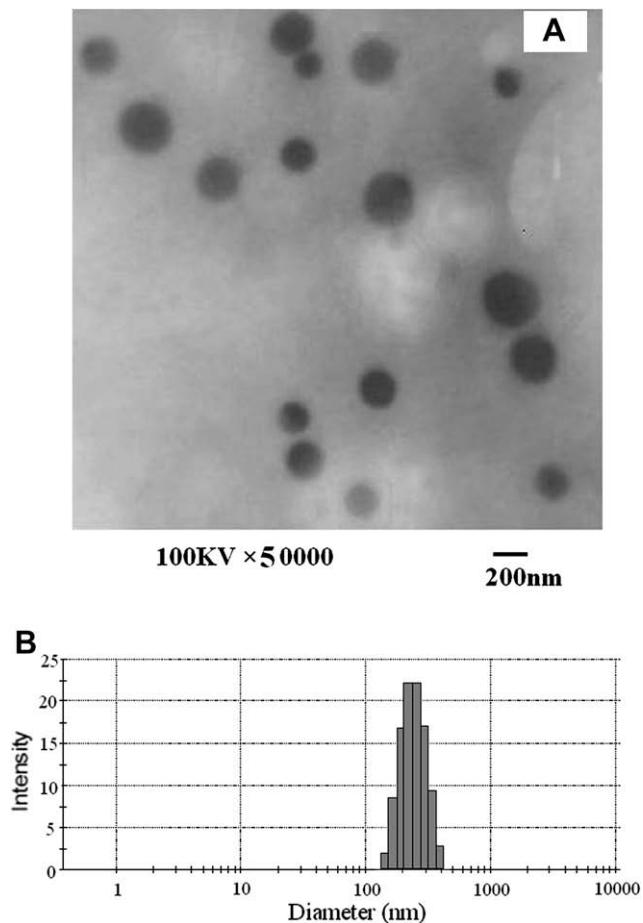


Figure 3. TEM image (A) and the particle size distributions (B) of QCS/poly (aspartic acid) nanoparticles (QCS = 2 mg/mL, poly (aspartic acid) = 1 mg/mL, QCS Mw = 65 kDa).

of QCS Mw and the pH of media on release of BSA are also discussed in the following sections.

2.2. Effects of the pH value of nanoparticles with different QCS/poly (aspartic acid) ratios

The zeta potentials of nanoparticles with different QCS/poly (aspartic acid) ratios in distilled water are listed in Table 1. When the content of poly (aspartic acid) increased, the pH values of the QCS/poly (aspartic acid) suspensions slowly decreased from 6.49 to 6.02. It was found that the zeta potential of pure QCS has a high positive charge (+65.9 mV). The QCS/poly (aspartic acid) nanoparticles also showed high positive values: their positive values of the zeta potential degraded as the content of poly (aspartic acid) increased. The result indicated that the QCS chains effectively cover the surface of the poly (aspartic acid) layers, and that an electrostatic interaction between QCS and poly (aspartic acid) has taken place.

Figure 4 illustrates that the BSA encapsulation efficiency increased with the increased pH value of nanoparticles with different QCS/poly (aspartic acid) ratios. The zeta potential of nanoparticles played important role in their drug encapsulation efficiency. The significantly increased nanoparticle zeta potential should be the main reason for the enhancement of BSA encapsulation efficiency along with the increased pH value of nanoparticles with different QCS/poly (aspartic acid) ratios. It is difficult to encapsulate BSA molecules completely within nanoparticles.³⁰ Hence, there must be a great part of BSA molecules absorbing around the surfaces of the nanoparticles, owing to the electrostatic interaction between the nanoparticles and BSA chains.³¹ In this way, for a certain weight of nanoparticles, high zeta potential of nanoparticles might absorb a larger amount of BSA than lower. Therefore, the increased BSA encapsulation efficiency along with the pH value of nanoparticles with different QCS/poly (aspartic acid) ratios may result from the increase in the zeta potential.

2.3. Effects of QCS Mw

The effects of QCS Mw on the average nanoparticle size, zeta potential, and nanoparticle yield (in Table 2), and on BSA encapsulation efficiency of QCS/poly (aspartic acid) nanoparticles (in Fig. 5) were investigated. As shown in Table 2, the average nanoparticle size increased as QCS Mw increased and the nanoparticles yield

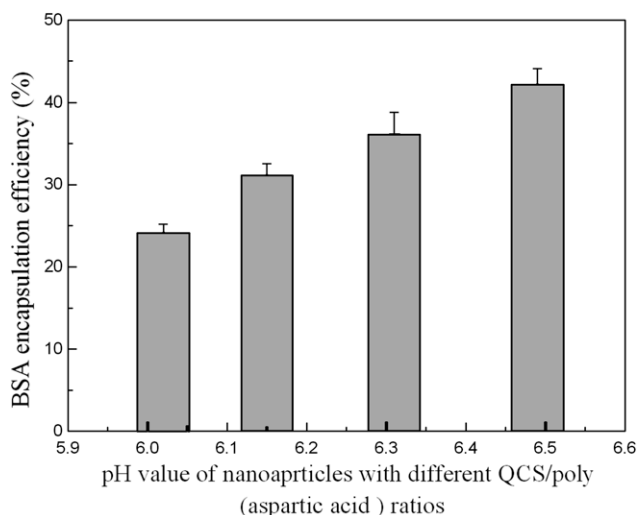


Figure 4. Effects of pH value of nanoparticles with different QCS/poly (aspartic acid) ratios on the BSA encapsulation efficiency (QCS Mw = 65 kDa, $n = 3$).

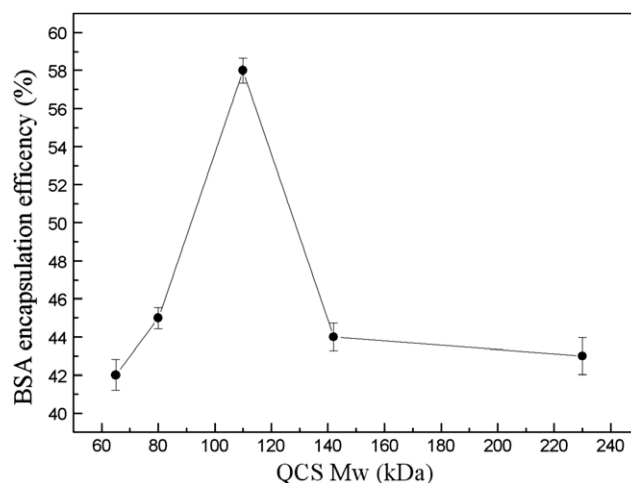


Figure 5. Effects of QCS Mw on the BSA encapsulation efficiency (QCS concentration = 2 mg/mL, poly (aspartic acid) concentration = 1 mg/mL, $n = 3$).

varied little along with QCS Mw, which meant similar nanoparticle formation ability regardless of the variation in QCS Mw. In Figure 5, it is shown that BSA encapsulation efficiency increased first and then decreased along with the gradual increase in QCS Mw.

The influence of CS Mw on encapsulation, some researchers believed that higher Mw of CS led to higher encapsulation efficiency because longer chain of CS molecule could entrap more BSA.^{29,30} The positive effect of high QCS Mw on BSA encapsulation was reasonable. On the other hand, QCS Mw also affected the size of the nanoparticles, as listed in Table 2. The size of the nanoparticles may further effect their BSA encapsulation, as discussed above. In this way, the enlargement of QCS/poly (aspartic acid) nanoparticles might lower BSA encapsulation efficiency due to the diminishment of total surface area. In view of the distinct effects of QCS Mw and nanoparticle size on BSA encapsulation, appropriate QCS Mw was necessary to obtain high BSA encapsulation efficiency.

2.4. Effects of QCS concentration

The influence of QCS concentration on encapsulation, it seemed that higher QCS concentration might contribute to higher encapsulation efficiency. However, it was reported that too high CS concentration made encapsulation extremely difficult.^{29,32} In our study, the reason for this problem might be revealed by investigating the nanoparticles yield.

Table 3 illustrates the effects of QCS concentration on the nanoparticle size, the nanoparticle yield, and Figure 6 illustrates the effects of QCS concentration on BSA encapsulation efficiency, respectively. In Table 3, it is shown that the nanoparticle size increased with the increase in QCS concentration. For example, when QCS concentration increased from 1 to 8 mg/mL, the nanoparticle size increased from 188 to 462 nm. However, the nanoparticle yield first increased a little and then decreased with the increase in QCS concentration (in Table 3). Meanwhile, BSA encapsulation efficiency increased within the QCS concentration range of 1–4 mg/mL and then decreased after that point (Fig. 6).

To explain the above phenomena, the formation mechanism of QCS/poly (aspartic acid) nanoparticles should be discussed. The formation of QCS/poly (aspartic acid) nanoparticles depended on the electrostatic interaction between negatively charged poly (aspartic acid) and positively charged QCS. In this process, poly (aspartic acid) acted as an ionic crosslinking reagent. In the crosslinking, there was an optimal ratio between QCS and poly (aspartic acid) to form the QCS/poly (aspartic acid) nanoparticles. In Table 3

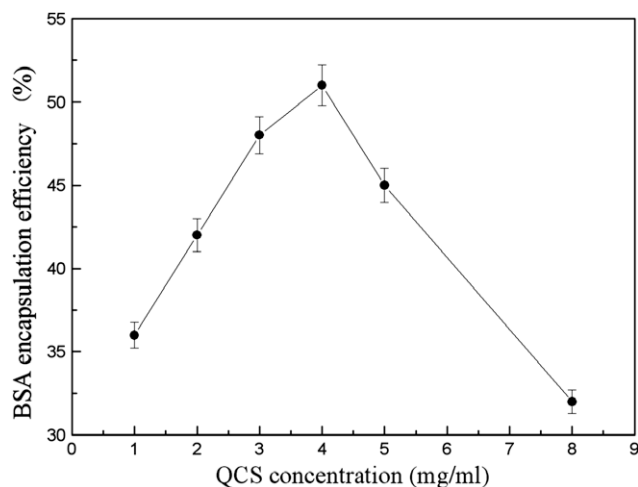


Figure 6. Effects of QCS concentrations on the BSA encapsulation efficiency (poly (aspartic acid) concentration = 1 mg/mL, QCS Mw = 65 kDa, $n = 3$).

it is shown that 2 mg/mL QCS versus 1 mg/mL poly (aspartic acid) should be the optimal ratio. Below the optimal ratio, the nanoparticle yield increased because the ratio between QCS and poly (aspartic acid) was nearing its optimality. Beyond the optimal ratio, with the fixed poly (aspartic acid) concentration, the ratio of poly (aspartic acid) to QCS lessened with increased QCS concentration and hence less nanoparticles formed. For this reason, moderate concentrations and ratios of poly (aspartic acid) and QCS were crucial to obtain a large amount of nanoparticles. In addition, with the increased QCS concentration, poly (aspartic acid) molecules in one nanoparticle could entangle with more QCS molecules so that the nanoparticles became larger and larger, as shown in Table 3.

For a certain type of nanoparticles, the encapsulation efficiency of BSA in QCS/poly (aspartic acid) nanoparticles gradually decreases with increasing QCS concentration due to the formation of less and less nanoparticles. However, BSA encapsulation efficiency increased with the QCS concentration from 1 to 4 mg/mL (Fig. 6). To explain this result, the property of BSA protein should be considered. At the isoelectric point of 4.5–4.8,³¹ BSA with negative charge could electrostatically interact with positive QCS. Thus, like poly (aspartic acid), BSA acted actually as another ionic cross-linking reagent. Therefore, the initial increase in BSA encapsulation efficiency in QCS/poly (aspartic acid) nanoparticles was reasonable within a certain range of QCS concentration, while the reduction in BSA encapsulation efficiency was inevitable when the nanoparticle yield continued to decrease, as illustrated in Figure 6 and Table 3.

2.5. Effects of poly (aspartic acid) concentration

From the above results and discussion, we found that the concentrations and ratio of poly (aspartic acid) and QCS were important to obtain a large amount of QCS/poly (aspartic acid) nanoparticles. Table 4 and Figure 7 displays the effects of poly (aspartic acid) concentration on the nanoparticle size, the nanoparticle yield, and BSA encapsulation efficiency, respectively. Table 4 illustrates that the nanoparticle size increased from 138 to 412 nm when poly (aspartic acid) concentration increased from 0.5 to 2 mg/mL. In addition, the nanoparticle yield increased significantly with increasing poly (aspartic acid) concentration (Table 4), meaning that the amount of the nanoparticles became larger and larger. Besides, BSA encapsulation efficiency increased within the poly (aspartic acid) concentration range of 0.5–2 mg/mL and QCS concentration 2 mg/mL. Above results illustrated that the in-

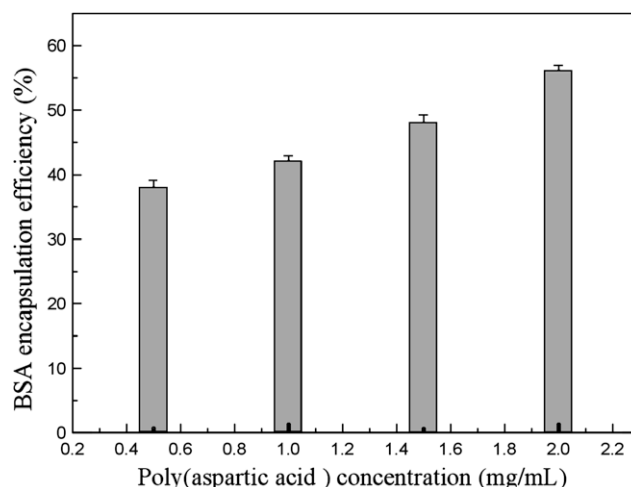


Figure 7. Effects of poly (aspartic acid) concentrations on the BSA encapsulation efficiency (QCS Mw = 65 kDa, $n = 3$).

creased nanoparticle yield contributed to the enhancement of BSA encapsulation efficiency (Table 4 and Fig. 7). It suggested that the increased nanoparticle yield played an important role in BSA encapsulation, although the enlarging nanoparticle size may have a negative effect on the BSA encapsulation. Obviously, increasing both poly (aspartic acid) and QCS concentrations at an optimal ratio was a good way to obtain a larger amount of the nanoparticles and a higher BSA encapsulation efficiency. However, the increase in poly (aspartic acid) and QCS concentrations was restricted to a certain extent. When poly (aspartic acid) concentration was over 2 mg/mL and QCS concentration was over 4 mg/mL some aggregates with large diameter formed.

2.6. Effects of BSA concentration

Effects of BSA concentration on particle size, polydispersity and zeta potential of BSA-loaded QCS/poly (aspartic acid) nanoparticles were further determined, as listed in Table 5. When the BSA concentration was increased, the size of the nanoparticles tended to decrease, and their zeta potential values were influenced little. Being a negatively charged macromolecule BSA may result in more efficient crosslinking and more compact structure of the nanoparticles, producing denser and smaller nanoparticles.³² In terms of the effect of BSA on zeta potential, it seemed that there was no direct correlation between the BSA concentration and the zeta potential of the nanoparticles.

2.7. In vitro release of BSA

In vitro release of BSA from the nanoparticles in both simulated gastric fluid (0.1 M HCl) and simulated intestinal fluid (0.1 M PBS, pH 7.4) at 37 °C was shown in Figure 8. The release profile was characterized by an initial burst effect followed by a continuous and slow release phase. As shown in Figure 8, the release of BSA from QCS/poly (aspartic acid) nanoparticles incubated in simulated intestinal fluid was much faster than that for nanoparticles incubated in simulated gastric fluid in the same period. Only 23% BSA was released in 0.1 M HCl, while more than 70% of BSA was eluted out in PBS from the nanoparticles. The accelerated release of BSA from QCS/ poly (aspartic acid) nanoparticles incubated in the high pH media was more likely owed to the reduced electrostatic interactions between the polyion complexes and the nanoparticles at this pH. The morphology of nanoparticles after 12 h immersion in 0.1 M HCl and 0.1 M PBS was shown in Figure 9. The morphology

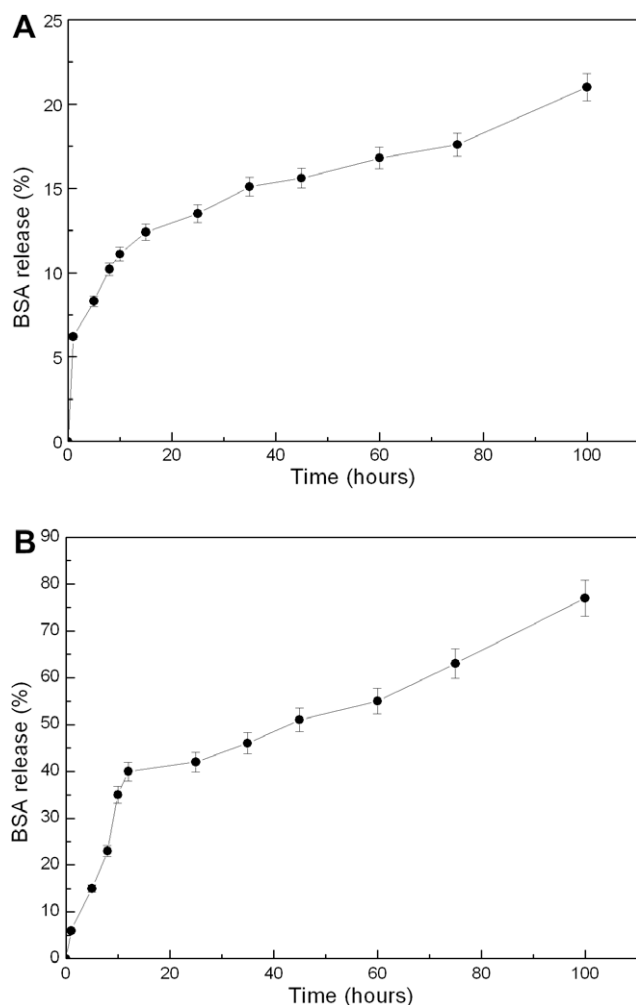


Figure 8. In vitro release of BSA from QCS/poly (aspartic acid) nanoparticles with different media of QCS (A) in 0.1 M HCl and (B) in 0.1 M PBS (pH 7.4) (QCS Mw = 65 kDa, $n = 3$).

of nanoparticles did not show observable change in acid medium (Fig. 9A). By contrast, irregular shape particles were found in PBS due to the disintegration of the poly (aspartic acid) matrix in the nanoparticles (Fig. 9B). Two processes could explain the release of a drug from a particle: diffusion and erosion. Therefore, in 0.1 M HCl, it seemed that the process of BSA release was mainly controlled by the diffusion process. In PBS, in addition to the diffusion process, the ion exchanges between polymer and release medium cause the erosion of the nanoparticles and greatly increase the BSA release rate.

3. Conclusion

In conclusion, novel QCS/poly (aspartic acid) nanoparticle system was successfully prepared via the ionotropic gelation method. Suitably pH value of nanoparticles with different QCS/ poly (aspartic acid) ratios, moderate QCS Mw, at an optimal ratio of poly (aspartic acid) concentration, and QCS concentration favored more nanoparticles yield and higher BSA encapsulation efficiency. The release of BSA from nanoparticles was pH-dependent. Quicker release was observed in PBS compared with that at low pH. The results showed that the new QCS/poly (aspartic acid) nanoparticles have a promising potential in protein-delivery system.

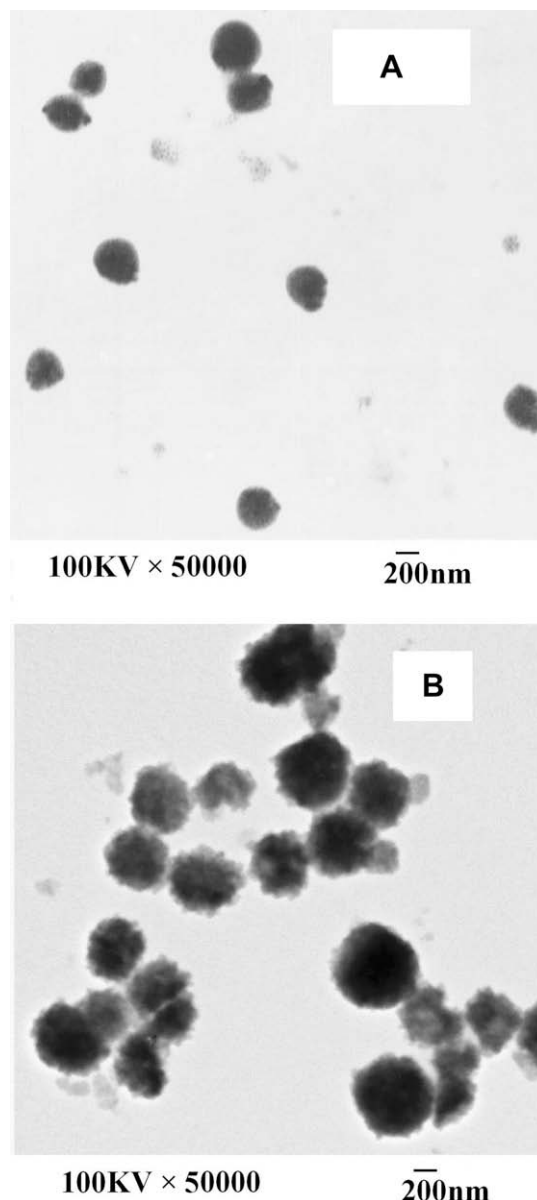


Figure 9. TEM of BSA loaded QCS/poly (aspartic acid) nanoparticles (A) in 0.1 M HCl and (B) in 0.1 M PBS for 12 h (QCS Mw = 65 kDa, 2.0 mg/mL, poly (aspartic acid) 1.0 mg/mL BSA 0.5 mg/mL).

4. Experimental

4.1. Materials and methods

Chitosan with the deacetylation degree (DD) of 90% and the molecular weight (Mw) of 360 kDa was purchased from Jinqiao Biochemistry (Zhejiang, China). The Mws were measured through the viscometric method while the DDs were determined by elemental analysis. Poly-L-aspartic acid sodium salt (Mw 5–15 kDa) was purchased from Sigma Chemical Co. (St. Louis, MO, USA). BSA with Mw of 66432.3 Da was purchased from Sigma Chemical (USA). All other reagents and solvents were of analytical grade.

4.2. Preparation of quaternary chitosan salt

The quaternary chitosan salt (QCS) was prepared by a modified method proposed by Spinelli et al.³³ Chitosan (1.5 g,

9.3 mmol) was dispersed in isopropyl alcohol (15.0 mL). Glycidyl trimethyl ammonium (5.65 g, 37.2 mmol) was dissolved in aqueous solution and added to chitosan suspension. The mol ratio of glycidyl trimethyl ammonium to amino groups of chitosan was 4. After reaction for 6 h at 80 °C, the reaction mixture was precipitated by acetone, dialyzed, and finally freeze-dried to obtain QCS, with molecular weight (M_w) of 230 kDa (determined by the GPC method) and the degree of substitution (DS) of 61% (determined by potentiometry). QCS with different M_w was obtained by H_2O_2 degradation. A given amount of QCS was dissolved in distilled water. Then a measured amount of H_2O_2 (30%, v/v) was added into the solution and stirred at 50 °C for 4 h. Samples were concentrated under reduced pressure. Weight-average molecular weights (M_w s) of QCS were measured by Gel permeation chromatography (GPC, Waters 2410 GPC apparatus (USA)).

4.3. Preparation of nanoparticles

QCS/poly (aspartic acid) nanoparticles were prepared via ionotropic gelation between the positively charged amino groups of QCS and the negatively charged poly (aspartic acid). Briefly, QCS was dissolved in water at various QCS concentrations. Three milliliters of an aqueous solution of poly (aspartic acid) (0.5–2 mg/mL) were added drop by drop to 6 mL of a QCS solution (1–8 mg/mL) with MW_s under magnetic stirring at room temperature. Magnetic stirring was maintained for 30 min to allow the complete stabilization of the system. The nanoparticles were isolated by ultracentrifugation at 20,000 rpm for 30 min at 4 °C.

The BSA-loaded nanoparticles were obtained by adding BSA into QCS solution before the addition of poly (aspartic acid).

4.4. Physicochemical characterization of QCS and QCS/poly (aspartic acid) nanoparticles

Chitosan and QCS were mixed with KBr and pressed to a plate for FTIR measurement. QCS nanoparticles were lyophilized and mixed with KBr to press a plate for measurement on a FTIR spectrum instrument (Perkin–Elmer, America).

The size and zeta potential of the colloidal systems were determined by photon correlation spectroscopy and laser Doppler anemometry using a Zetasizer 3000 HS (Malvern Instruments, Malvern, United Kingdom). Each batch was analyzed in triplicate.

TEM (CM12 Philips, Eindhoven, Netherlands) was used to observe the morphology of nanoparticles. Samples were stained with 2% (w/v) phosphotungstic acid and dried on copper grill at room temperature.

4.5. Determination of nanoparticle yield and BSA encapsulation efficiency

The encapsulation efficiencies of BSA in QCS/poly (aspartic acid) nanoparticles with different formations were determined by ultra-centrifuging the nanoparticles suspension at 20,000 rpm at 4 °C for 30 min. The precipitate separated from the supernatant was dried at 70 °C for 12 h and weighed. The amount of free BSA in supernatant was determined by UV spectrophotometry at 595 nm using a Bradford protein assay.³⁴ The yield of the nanoparticles was dry weight of nanoparticle precipitate. The BSA encapsulation efficiency (AE) in the nanoparticles was calculated as follows:

$$AE = [(total\ BSA - free\ BSA) / total\ BSA] \times 100$$

All measurements were performed in triplicate.

4.6. In vitro release studies

About 25 mg of the dried BSA-loaded nanoparticles was suspended in 5 mL of 0.1 mol/L HCl or 0.1 mol/L PBS of pH 7.4, stabilized with 0.2% NaN₃ (w/v), and then incubated at 37 °C under stirring at the rate of 120 rpm on the SHZ-88 Constant Temperature Water-bath Shaker (China). At predetermined intervals, samples were ultracentrifuged. Two milliliters of the supernatant were taken out and the free BSA was determined by protein assay as described earlier. The calibration curve was made using non-loaded BSA nanoparticles as correction. Each experiment was repeated thrice and the result was the mean value of three samples. The error bars in the plot showed the standard deviation of data.

Acknowledgments

This project was supported by the National High Technology Research and Development Program of China (863) (No: 2006AA03Z321); the major program for fundamental research of the Chinese academy of sciences, China (No: KJXC2-YW-M02); the State Key Development Program for Basic Research of China (973) (No: 2009CB930200).

References

- Sood, A.; Panchagnula, R. *Chem. Rev.* **2001**, *101*, 3275–3303.
- Yasui, K.; Nakamura, Y. *Biol. Pharm. Bull.* **2000**, *3*, 218–322.
- Russell-Jones, G. J. *J. Controlled Release* **2000**, *65*, 49–54.
- Liu, Y.; Guo, L. K.; Huang, L.; Deng, X. M. *J. Appl. Polym. Sci.* **2003**, *90*, 3150–3156.
- Aboubakar, M.; Couvreur, P.; Pinto-Alphandary, H.; Gouritin, B.; Lacour, B.; Farinotti, R.; Puisieux, F.; Vauthier, C. *Drug Dev. Res.* **2000**, *49*, 109–117.
- Ydens, I.; Rutot, D.; Degee, P.; Six, J.; Dellacherie, E.; Dubois, P. *Macromolecules* **2000**, *33*, 6713–6721.
- Ma, J. B.; Cao, H. H.; Li, Y. H.; Li, X. J. *Biomater. Sci., Polym. Ed.* **2002**, *13*, 67–80.
- Tobio, M.; Sánchez, A.; Vila, A.; Soriano, I.; Evora, C.; Vila-Jato, J. L.; Alonso, M. J. *Colloids Surf., B: Biointerface* **2000**, *18*, 315–323.
- Ravi Kumar, M. N. V.; Bakowsky, U.; Lehr, C. M. *Biomaterials* **2004**, *25*, 1771–1777.
- Fonseca, C.; Simoes, S.; Gaspar, R. J. *Controlled Release* **2002**, *3*, 273–286.
- Yong, H.; Xiqun, J.; Yin, D.; Haixiong, G.; Yuyan, Y.; Changzheng, Y. *Biomaterials* **2002**, *23*, 3193–3201.
- Park, J. S.; Cho, Y. W. *Macromol. Res.* **2007**, *15*, 513–519.
- Owman, K.; Leong, K. W. *Int. J. Nanomed.* **2006**, *1*, 117–128.
- Agnihotri, S. A.; Aminabhavi, T. M. *Drug Dev. Ind. Pharm.* **2007**, *33*, 1254–1262.
- Yamada, S.; Ganno, T.; Ohara, N.; Hayashi, Y. J. *Biomed. Mater. Res. Part A* **2007**, *83A*, 290–295.
- Fernández-Urrusuno, R.; Romani, D.; Calvo, P.; Vila-Jato, J. L.; Alonso, M. J. *S. T. P. Pharm. Sci.* **1999**, *9*, 429–436.
- Fernández-Urrusuno, R.; Calvo, P.; Remu-nan-Lopez, C.; Vila-Jato, J. L.; Alonso, M. J. *Pharm. Res.* **1999**, *16*, 1576–1581.
- Vila, A.; Sánchez, A.; Janes, K. A.; Behrens, I.; Kissel, T.; Vila-Jato, J. L.; Alonso, M. J. *Eur. J. Pharm. Biopharm.* **2004**, *57*, 123–132.
- Qu, X.; Wirsén, A.; Albertsson, A. C. *Polymer* **2000**, *41*, 4841–4847.
- MacLaughlin, I. C.; Mumper, R. J.; Wang, J.; Tagliaferri, J. M.; Gill, I.; Hinchclife, M.; Rolland, A. P. *J. Controlled Release* **1998**, *56*, 259–272.
- Thanou, M.; Verhoef, J. C.; Junginger, H. E. *Adv. Drug Delivery Rev.* **2001**, *52*, 117–126.
- Vander Merwe, S. M.; Verhoef, J. C.; Verheijden, J. H.; Kotze, A. F.; Junginger, H. E. *Eur. J. Pharm. Biopharm.* **2004**, *58*, 222–235.
- Amadd, W.; Amass, A. A.; Tighe, B. *Polym. Int.* **1998**, *47*, 89–144.
- Yokoyama, M.; Okano, T.; Sakurai, Y.; Kataoka, K. *J. Controlled Release* **1994**, *32*, 269–277.
- Bae, Y.; Fukushima, S.; Harada, A.; Kataoka, K. *Angew. Chem., Int. Ed.* **2003**, *42*, 4640–4643.
- Prompruk, K.; Govender, T.; Zhang, S.; Xiong, C. D.; Stolnik, S. *Int. J. Pharm.* **2005**, *297*, 242–253.
- Arimura, H.; Ohya, Y.; Ouchi, T. *Biomacromolecules* **2005**, *6*, 720–725.
- Arimura, H.; Ohya, Y.; Ouchi, T. *Macromol. Rapid Commun.* **2004**, *25*, 743–747.
- Wu, Y.; Yang, W. L.; Wang, C. C.; Hu, J. H.; Fu, S. K. *Int. J. Pharm.* **2005**, *295*, 235–245.
- Xu, Y. M.; Du, Y. M. *Int. J. Pharm.* **2003**, *250*, 215–226.
- Calvo, P.; Remunán-López, C.; Vila-Jato, J. L.; Alonso, M. J. *Pharm. Res.* **1997**, *14*, 1431–1436.
- Zhang, H.; Megan, O.; Christine, A.; Eugenia, K. *Biomacromolecules* **2004**, *5*, 2461–2468.
- Spinelli, V. A.; Laranjeira, M. C. M.; Fa'vere, V. T. *React. Funct. Polym.* **2004**, *61*, 347–352.
- John, M. W. *The Protein Protocols Handbook*; Humana: Totowa, NJ, 2002. p 15.